HAL open science

Recursive subspace identification for in flight modal analysis of airplanes

Katrien de Cock, Guillaume Mercère, Bart de Moor

To cite this version:

Katrien de Cock, Guillaume Mercère, Bart de Moor. Recursive subspace identification for in flight modal analysis of airplanes. International Conference on Noise and Vibration Engineering, ISMA 2006, Sep 2006, Leuven, Belgium. pp.CDROM. hal-00097999

HAL Id: hal-00097999

https://hal.science/hal-00097999v1

Submitted on 23 Sep 2006

HAL is a multi-disciplinary open access archive for the deposit and dissemination of scientific research documents, whether they are published or not. The documents may come from teaching and research institutions in France or abroad, or from public or private research centers.

L'archive ouverte pluridisciplinaire **HAL**, est destinée au dépôt et à la diffusion de documents scientifiques de niveau recherche, publiés ou non, émanant des établissements d'enseignement et de recherche français ou étrangers, des laboratoires publics ou privés.

Recursive subspace identification for in-flight modal analysis of airplanes

Katrien De Cock[1*], **Guillaume Mercère**[2†] **and Bart De Moor**[1‡]
[1] K.U.Leuven, Dept. of Electrical Engineering (ESAT–SCD)
Kasteelpark Arenberg 10, B-3001, Leuven, Belgium
e-mail: **katrien.decock@esat.kuleuven.be**
[2] Laboratoire d'Automatique et d'Informatique Industrielle
40, avenue du recteur Pineau, 86022 Poitiers, France

Abstract
In this paper recursive subspace identification algorithms are applied to track the modal parameters of airplanes on-line during test flights. The ability to track changes in the damping ratios and the influence of the forgetting factor are studied through simulations.

1 Introduction

The development of new aircraft requires a careful exploration of the dynamical behavior of the structure subject to vibration and aero-elastic forces. This is achieved via a combination of ground and in-flight tests. The objective of the in-flight tests is to determine the structural dynamic state for selected flight configurations (constant speed and attitude) and to validate the aero-elastic model in flight.
Linear system identification is an important tool in this experimental modal analysis. A linear model for the airplane is estimated based on the available observations. From the model, modal characteristics as resonance frequencies, damping ratios and mode shapes are extracted. Subspace identification algorithms allow for a fast and robust identification of multi-input multi-output (MIMO) systems by using projections of subspaces spanned by the rows of block Hankel matrices containing input and output measurements.
Because test flights are expensive, a fast analysis of the test data is very important. Until now, off-line processing of the data is performed. A batch of data samples is collected and used to estimate the model parameters. While processing the data, the pilot has to wait for instructions. On-line and in-flight exploitation of the data would allow a more direct exploration of the flight domain, with improved confidence and reduced costs.
In this paper, recently proposed recursive subspace identification algorithms [12–14] are applied for on-line tracking of the modal parameters of the airplane. At every time instant, the estimates of the parameters are updated. Besides the faster processing of the data, a recursive algorithm also reduces the constraints on the amount of data that can be processed so that more sensors can be used. Moreover, it can be used to detect changes in the dynamics of the linear model, e.g. the on-set of flutter, which happens when the damping of some mode becomes too small. It is also able to cope with time varying characteristics resulting from flight test conditions.
Several types of data sets are available from flight tests. Some consist only of output data, when only the excitations by e.g. wind and turbulence, which are not measured, are used. For these, the recursive stochastic

[*] Dr. Katrien De Cock is a postdoctoral researcher at the K.U.Leuven, Belgium.
[†] Dr. Guillaume Mercère is an assistant professor at the Laboratoire d'Automatique et d'Informatique Industrielle, Poitiers, France.
[‡] Dr. Bart De Moor is a full professor at the K.U.Leuven, Belgium.

subspace identification algorithm in [5] can be applied. In other data sets, known excitations (e.g. from the fly-by-wire control system) and unknown excitations are present. In this paper, we deal with the latter kind of data. The recently proposed recursive subspace identification methods by Mercère et al. [12–14], which are suited for these data types, are applied to data from test flights and the results are shown. The ability to track changes in the damping (slowly varying damping coefficients as well as abrupt changes) and the influence of the forgetting factor are studied on simulated data.
The remainder of this paper is organized as follows. In Section 2 the identification problem is formulated. In Section 3 subspace identification algorithms are briefly described. Recursive versions of subspace identification are discussed in Section 4. Section 5 contains simulation examples and Section 6 applications of the methods to data from flight tests. Section 7 gives conclusions and describes our future work.

2 Problem formulation

In this paper, discrete time, linear time-invariant models with the following state space representation are considered

$$\left\{ \begin{array}{rcl} x_{k+1} & = & Ax_k + Bu_k + w_k \,, \\ y_k & = & Cx_k + Du_k + v_k \,, \end{array} \right. \quad \text{with } \mathbf{E}\left[\begin{pmatrix} w_p \\ v_p \end{pmatrix} \begin{pmatrix} w_q^T & v_q^T \end{pmatrix} \right] = \begin{pmatrix} Q & S \\ S^T & R \end{pmatrix} \delta_{pq} \quad \geq 0 \,,$$

where $u_k \in \mathbb{R}^m$ and $y_k \in \mathbb{R}^l$ are the observations at time instant k of respectively the m inputs and l outputs of the process, $\mathbf{E}$ denotes the expected value operator and δ_{pq} the Kronecker delta. The vector $x_k \in \mathbb{R}^n$ is the state vector of the process at discrete time instant k and contains the numerical values of n states. $v_k \in \mathbb{R}^l$ and $w_k \in \mathbb{R}^n$ are unobserved vector signals, usually called the measurement, respectively process noise. It is assumed that they are zero mean, stationary, white noise vector sequences. The matrix pair $\{A, C\}$ is assumed to be observable, which implies that all modes in the system can be observed in the output y_k and can thus be identified. The matrix pair $\{A, [\ B \quad Q^{1/2}\ ]\}$ is assumed to be controllable, which in its turn implies that all modes of the system can be excited by either the deterministic input u_k and/or the stochastic input w_k.
In modal analysis applications, the modal parameters are extracted from the state space model. First, an eigenvalue decomposition is applied to the dynamical system matrix A: $A = \Psi\Lambda\Psi^{-1}$, where $\Psi \in \mathbb{C}^{n\times n}$ is the eigenvector matrix and $\Lambda \in \mathbb{C}^{n\times n}$ is the diagonal eigenvalue matrix (assuming A to be diagonalizable). The matrix Λ contains the n discrete-time eigenvalues μ_i, of which the complex conjugated pairs contribute to the vibration modes. They are related to the continuous-time eigenvalues λ_i as $\mu_i = e^{\lambda_i T_s}$ where T_s is the sampling time (sampling frequency $f_s = \frac{1}{T_s}$). The resonance frequencies f_i and damping ratios ζ_i can then be found from $\lambda_i, \lambda_i^* = -\zeta_i f_i \pm j\sqrt{(1-\zeta_i^2)}\ f_i$.
In this paper the resonance frequencies f_i and damping ratios ζ_i are tracked on-line, given the input and output measurements u_k and y_k. A subspace identification algorithm is used to obtain an initial model, which is then updated every time a new input-output measurement is made.

3 Subspace identification for modal analysis

Subspace identification algorithms have gained increasing attention in the modal analysis community over the last few years, see for instance [1, 3, 8, 17]. This is due to their inherent numerical robustness and their ability to deal with large numbers of inputs and outputs. In contrast to classical predictor error methods, where a costly, often nonlinear optimization has to be performed, subspace identification techniques derive models for linear systems solely by applying well-conditioned operations like LQ and singular value decompositions on block Hankel data matrices.
Block Hankel matrices with input and output data are the basic starting blocks for subspace identification

algorithms. Input block Hankel matrices are defined as follows

$$U = \left(\begin{array}{ccccc} u_1 & u_2 & u_3 & \cdots & u_j \\ u_2 & u_3 & u_4 & \cdots & u_{j+1} \\ \vdots & \vdots & \vdots & \cdots & \vdots \\ u_i & u_{i+1} & u_{i+2} & \cdots & u_{i+j-1} \\ \hline u_{i+1} & u_{i+2} & u_{i+3} & \cdots & u_{i+j} \\ u_{i+2} & u_{i+3} & u_{i+4} & \cdots & u_{i+j+1} \\ \vdots & \vdots & \vdots & \cdots & \vdots \\ u_{2i} & u_{2i+1} & u_{2i+2} & \cdots & u_{2i+j-1} \end{array}\right) = \left(\begin{array}{c} U_p \\ \hline U_f \end{array}\right) ,$$

where the number of block rows i in U_p and U_f is a user-defined index, which is large enough, i.e. $il \geq n$, the number of columns j is typically equal to $s - 2i + 1$, where s is the number of available data samples. The subscript 'p' stands for 'past' and the subscript 'f' for 'future'. The output block Hankel matrices Y, Y_p, Y_f are defined in a similar way.
The MOESP algorithms [21, 23–25], on which most recursive subspace identification methods are based, start from the so called past and future data equations [26]

$$\begin{aligned} Y_p &= \Gamma_i X_p + H_i U_p + N_p \\ Y_f &= \Gamma_i X_f + H_i U_f + N_f \ , \end{aligned}$$

where $\Gamma_i = \begin{pmatrix} C^T & (CA)^T & \cdots & (CA^{i-1})^T \end{pmatrix}^T \in \mathbb{R}^{li \times n}$ is the extended observability matrix, X_p (respectively X_f) is a past (respectively future) state sequence, H_i is the block Toeplitz matrix of the (unknown) impulse response from u to y and N_p (respectively N_f) a particular combination of the past (respectively future) block Hankel matrices of the perturbations v and w. For simultaneously removing the term $H_i U_f$ from Y_f and decorrelating the noise, it is proposed to consider the following quantity: $Y_f \Pi_{U_f^\perp} \Xi_p$, where Ξ_p is an instrumental variable composed by past input (and output) data and where[1] $\Pi_{U_f^\perp} = I_j - U_f^T (U_f U_f^T)^\dagger U_f$. Indeed, it can be proved that, under particular rank and excitation conditions [21]

$$\lim_{s \to \infty} \frac{1}{s} Y_f \Pi_{U_f^\perp} \Xi_p = \lim_{s \to \infty} \frac{1}{s} \Gamma_i X_f \Pi_{U_f^\perp} \Xi_p \ ,$$

with s the number of data points. This data compression can be efficiently computed by means of the following LQ decomposition[2]

$$\begin{pmatrix} U_f \\ \Xi_p \\ Y_f \end{pmatrix} = \begin{pmatrix} L_{11} & 0 & 0 \\ L_{21} & L_{22} & 0 \\ L_{31} & L_{32} & L_{33} \end{pmatrix} \begin{pmatrix} Q_1^T \\ Q_2^T \\ Q_3^T \end{pmatrix} \tag{1}$$

since $\lim_{s \to \infty} \frac{1}{s} \text{span}_{\text{col}} \{L_{32}\} = \text{span}_{\text{col}} \{\Gamma_i\}$. The estimation of the observability matrix is then realized by considering the following SVD

$$L_{32} = \begin{pmatrix} U_1 & U_2 \end{pmatrix} \begin{pmatrix} S_1 & 0 \\ 0 & S_2 \end{pmatrix} \begin{pmatrix} V_1 & V_2 \end{pmatrix}^T \ ,$$

where $U_1 \in \mathbb{R}^{il \times n}$, $S_1 \in \mathbb{R}^{n \times n}$ and $V_1 \in \mathbb{R}^{j \times n}$. An estimate for the matrices A and C, up to a similarity transformation, can then be obtained as follows: $\hat{C}$ is equal to the first l rows of U_1 and $\hat{A}$ is equal to $\underline{U_1}^\dagger \overline{U_1}$, with $\underline{U_1}$ and $\overline{U_1}$ shorthand notations for U_1 with its last, respectively first l lines removed. This MOESP scheme is named PI MOESP when $\Xi_p = U_p$ and PO MOESP when $\Xi_p = \begin{pmatrix} U_p^T & Y_p^T \end{pmatrix}^T$ [21].

[1] $\bullet^\dagger$ denotes the Moore-Penrose pseudo-inverse of the matrix $\bullet$.
[2] The LQ decomposition of a matrix A is the transpose of the QR decomposition of A^T.

4 Recursive subspace identification

As introduced previously, one of the reasons for the success of subspace model identification (SMI) techniques lies in the direct correspondence between geometric operations on matrices constructed from input-output data and their implementation in terms of well known, stable and reliable algorithms from the field of numerical linear algebra. However, most of the available batch SMI techniques are based on tools such as the SVD which are not suitable for online implementation due to their computational complexity. Several recursive subspace identification algorithms have been proposed during the last years [2, 5, 7, 10, 12, 14, 16, 22] to avoid the use of such burdensome tools. More precisely, most recent recursive algorithms circumvent this problem by considering the similarities between recursive subspace identification and adaptive signal processing techniques for direction of arrival estimation [9], such as the projection approximation subspace tracking technique [27] and the propagator method [15].
Because we are concerned with the recursive estimation of the resonance frequencies and the damping ratios, we will concentrate on the estimation of the matrices A and C and will not deal with the estimation of B and D. Therefore, only the extended observability matrix Γ_i needs to estimated recursively from the updates of the input-output data u and y. To this purpose, consider the block Hankel matrices U_p, U_f, Y_p and Y_f and assume that, at time $s+1$, new data samples y_{s+1} and u_{s+1} are acquired. Then, each of the block Hankel matrices is modified by the addition of a column

$$\mathrm{u}_{p,s+1} = \begin{pmatrix} u_{j+1}^T & \cdots & u_{i+j}^T \end{pmatrix}^T \in \mathbb{R}^{mi\times 1} \qquad \mathrm{y}_{p,s+1} = \begin{pmatrix} y_{j+1}^T & \cdots & y_{i+j}^T \end{pmatrix}^T \in \mathbb{R}^{li\times 1}$$
$$\mathrm{u}_{f,s+1} = \begin{pmatrix} u_{i+j+1}^T & \cdots & u_{2i+j}^T \end{pmatrix}^T \in \mathbb{R}^{mi\times 1} \qquad \mathrm{y}_{f,s+1} = \begin{pmatrix} y_{i+j+1}^T & \cdots & y_{2i+j}^T \end{pmatrix}^T \in \mathbb{R}^{li\times 1} .$$

Then, it is easy to show that

$$\mathrm{y}_{p,s+1} = \Gamma_i x_{j+1} + H_i \mathrm{u}_{p,s+1} + \mathrm{n}_{p,s+1}$$
$$\mathrm{y}_{f,s+1} = \Gamma_i x_{i+j+1} + H_i \mathrm{u}_{f,s+1} + \mathrm{n}_{f,s+1} ,$$

where the past and future stacked noise vectors are defined in the same way as, e.g. $\mathrm{u}_{p,s+1}$ and $\mathrm{u}_{f,s+1}$.
Recursive subspace identification algorithms consist, as their batch counterparts, of two steps. First, the data compression phase is updated. This can be done by updating the LQ decomposition (1) by means of Givens rotations [6], as described in [10, 12]. Second, the column space of Γ_i is updated. This is usually done by solving a minimization problem [5, 7, 10, 12, 16] in order to avoid an SVD.
Two recursive subspace identification methods are considered in more detail in the following. The first method, named `RPM2`, is described in Section 4.1. The second one, called `EIVPM` [13], is given in Section 4.2.

4.1 RPM2

The first idea in this algorithm is to update the LQ factorization (see Equation (1)) of the PI/PO schemes by means of Givens rotations. For that purpose, assume that, at time $s+1$, a new set of input-output data vectors becomes available. Then, a new column is added to the data matrices and the decomposition must be written as

$$\begin{pmatrix} U_f & \mathrm{u}_{f,s+1} \\ \Xi_p & \xi_{p,s+1} \\ Y_f & \mathrm{y}_{f,s+1} \end{pmatrix} = \begin{pmatrix} L_{11,s} & 0 & 0 & \mathrm{u}_{f,s+1} \\ L_{21,s} & L_{22,s} & 0 & \xi_{p,s+1} \\ L_{31,s} & L_{32,s} & L_{33,s} & \mathrm{y}_{f,s+1} \end{pmatrix} \begin{pmatrix} Q_{1,s} & 0 \\ Q_{2,s} & 0 \\ Q_{3,s} & 0 \\ 0 & 1 \end{pmatrix} ,$$

where $\xi_{p,s+1} = \mathrm{u}_{p,s+1}$ for PI MOESP and $\xi_{p,s+1} = \begin{pmatrix} \mathrm{u}_{p,s+1}^T & \mathrm{y}_{p,s+1}^T \end{pmatrix}^T$ for PO MOESP. Givens rotations are then used twice to update this factorization. They are first applied in order to zero out the elements of vector $\mathrm{u}_{f,s+1}$, bringing the L factor to the form

$$\begin{pmatrix} L_{11,s+1} & 0 & 0 & 0 \\ L_{21,s+1} & L_{22,s} & 0 & \bar{\mathrm{z}}_{p,s+1} \\ L_{31,s+1} & L_{32,s} & L_{33,s} & \bar{\mathrm{z}}_{f,s+1} \end{pmatrix} .$$

Subsequently, the elements of $\bar{z}_{p,s+1}$ are zeroed in a similar way, to give

$$\begin{pmatrix} L_{11,s+1} & 0 & 0 & 0 \\ L_{21,s+1} & L_{22,s+1} & 0 & 0 \\ L_{31,s+1} & L_{32,s+1} & L_{33,s} & \bar{\bar{z}}_{f,s+1} \end{pmatrix}.$$

Then it is easy to show that the "square" of block $L_{32,s+1}$ can be written as [10, 12]

$$L_{32,s+1}L_{32,s+1}^T = L_{32,s}L_{32,s}^T + \bar{z}_{f,s+1}\bar{z}_{f,s+1}^T - \bar{\bar{z}}_{f,s+1}\bar{\bar{z}}_{f,s+1}^T \,.$$

Thus, in this case, the subspace estimate at time $s+1$ is related to the one at time s via the combination of an update and a downdate. Furthermore, by denoting $R_{z_f} = \mathbf{E}\left\{\bar{z}_{f,s+1}\bar{z}_{f,s+1}^T - \bar{\bar{z}}_{f,s+1}\bar{\bar{z}}_{f,s+1}^T\right\}$, it holds that [11]

$$R_{z_f} = \Gamma_i \mathbf{E}\left\{x_{i+j+1}x_{i+j+1}^T\right\}\Gamma_i^T = \Gamma_i R_x \Gamma_i^T.$$

The second step of this recursive subspace method consists in the online update of the observability matrix. In this paper, the focus will be on algorithms based on the propagator concept [15]. More precisely, under the assumption that the pair $\{A, C\}$ is observable, since $\Gamma_i \in \mathbb{R}^{li\times n}$ with $li > n$, the extended observability matrix has n linearly independent rows, which can be gathered in a submatrix Γ_{i_1}. Then, the complement Γ_{i_2}, i.e. the matrix consisting of the rows of Γ_i that are not in Γ_{i_1}, can be expressed as a linear combination of the n rows in Γ_{i_1}. So, there is a unique linear operator $P \in \mathbb{R}^{n\times(li-n)}$, named propagator [15], such that $\Gamma_{i_2} = P^T\Gamma_{i_1}$. Furthermore, it is easy to verify that $\Gamma_i = \begin{pmatrix} I_n \\ P^T \end{pmatrix}\Gamma_{i_1}$. Thus, since rank $\{\Gamma_{i_1}\} = n$,

$$\text{span}_{\text{col}}\{\Gamma_i\} = \text{span}_{\text{col}}\left\{\begin{pmatrix} I_n \\ P^T \end{pmatrix}\right\}. \tag{2}$$

Equation (2) implies that it is possible to estimate the observability matrix (in a particular basis) by estimating the propagator. For that purpose, consider the following partitions:

$$\bar{z}_{f,s+1} = \begin{pmatrix} \bar{z}_{f_1,s+1} \\ \bar{z}_{f_2,s+1} \end{pmatrix} \text{ and } \bar{\bar{z}}_{f,s+1} = \begin{pmatrix} \bar{\bar{z}}_{f_1,s+1} \\ \bar{\bar{z}}_{f_2,s+1} \end{pmatrix},$$

where $\bar{z}_{f_1,s+1} \in \mathbb{R}^{n\times 1}$ (respectively $\bar{\bar{z}}_{f_1,s+1}$) and $\bar{z}_{f_2,s+1} \in \mathbb{R}^{(li-n)\times 1}$ (respectively $\bar{\bar{z}}_{f_2,s+1}$) are the components of $\bar{z}_{f,s+1}$ (respectively $\bar{\bar{z}}_{f,s+1}$) corresponding to Γ_{i_1} and Γ_{i_2}. Then, it is straightforward to show that[3]

$$\hat{P}^T = \left(R_{\bar{z}_{f_2}\bar{z}_{f_1}} - R_{\bar{\bar{z}}_{f_2}\bar{\bar{z}}_{f_1}}\right)\left(R_{\bar{z}_{f_1}} - R_{\bar{\bar{z}}_{f_1}}\right)^{-1}.$$

This estimated matrix corresponds to the optimum of the following cost function

$$J(P) = \mathbf{E}\left\|\bar{z}_{f_2} - P^T\bar{z}_{f_1}\right\|^2 - \mathbf{E}\left\|\bar{\bar{z}}_{f_2} - P^T\bar{\bar{z}}_{f_1}\right\|^2,$$

the minimization of which is given by the following recursive algorithm[4]

$$\begin{aligned}
\underline{L}_{f,s+1} &= \frac{1}{\lambda}\left(\underline{\underline{L}}_{f,s} - \frac{\underline{\underline{L}}_{f,s}\bar{z}_{f_1,s+1}\bar{z}_{f_1,s+1}^T\underline{\underline{L}}_{f,s}}{\lambda + \bar{z}_{f_1,s+1}^T\underline{\underline{L}}_{f,s}\bar{z}_{f_1,s+1}}\right) \\
\underline{\underline{L}}_{f,s+1} &= \underline{L}_{f,s+1} + \frac{\underline{L}_{f,s+1}\bar{\bar{z}}_{f_1,s+1}\bar{\bar{z}}_{f_1,s+1}^T\underline{L}_{f,s+1}}{1 - \bar{\bar{z}}_{f_1,s+1}^T\underline{L}_{f,s+1}\bar{\bar{z}}_{f_1,s+1}} \\
P_{s+1}^T &= P_s^T + \left(\bar{z}_{f_2,s+1} - P_s^T\bar{z}_{f_1,s+1}\right)\bar{z}_{f_1,s+1}^T\underline{\underline{L}}_{f,s+1} - \left(\bar{\bar{z}}_{f_2,s+1} - P_s^T\bar{\bar{z}}_{f_1,s+1}\right)\bar{\bar{z}}_{f_1,s+1}^T\underline{\underline{L}}_{f,s+1}.
\end{aligned}$$

[3]The following notation is used for covariance matrices: $\mathbf{E}\left\{ab^T\right\} = R_{ab}$, with $R_{aa} = R_a$.

[4]λ is a forgetting factor introduced to weight the past information.

4.2 EIVPM

In order to improve the computational complexity of the previous method (see Subsection 6.3 for a case study and [11] for a theoretical analysis), it is proposed hereafter to introduce another recursive subspace algorithm. Although also based on the propagator approach, the developed method rests on the recursive update of the LQ factorization of an other MOESP scheme: ordinary MOESP [24]. On the contrary to the PI/PO MOESP schemes, the ordinary MOESP identification method only uses the following data equation

$$Y_f = \Gamma_i X_f + H_i U_f + N_f \ ,$$

but leads to consistent estimates of the observability matrix if $w = 0$ and v is a white Gaussian noise [24]. Even if this assumption seems to be too restrictive in the practical framework considered in this paper, the update of the ordinary MOESP LQ factorization will decrease the global computational load of the recursive algorithm and, as proved in [14], the noise treatment can be considered in the propagator estimation step by introducing instrumental variables.
Thus, consider the following classical LQ decomposition of the Ordinary MOESP [24]

$$\begin{pmatrix} U_f \\ Y_f \end{pmatrix} = \begin{pmatrix} L_{11,s} & 0 \\ L_{21,s} & L_{22,s} \end{pmatrix} \begin{pmatrix} Q_{1,s} \\ Q_{2,s} \end{pmatrix} .$$

When a new input-output couple is acquired, this decomposition can be updated as

$$\begin{pmatrix} U_f & \mathrm{u}_{f,s+1} \\ Y_f & \mathrm{y}_{f,s+1} \end{pmatrix} = \begin{pmatrix} L_{11,s} & 0 & \mathrm{u}_{f,s+1} \\ L_{21,s} & L_{22,s} & \mathrm{y}_{f,s+1} \end{pmatrix} \begin{pmatrix} Q_{1,s} & 0 \\ Q_{2,s} & 0 \\ 0 & 1 \end{pmatrix} .$$

A sequence of Givens rotations [6] can then be used to annihilate the stacked input vector $\mathrm{u}_{f,s+1}$ and bring back the L factor to the following block lower triangular form

$$\begin{pmatrix} L_{11,s+1} & 0 & 0 \\ L_{21,s+1} & L_{22,s+1} & \mathrm{z}_{f,s+1} \end{pmatrix} .$$

Then, it is possible to prove that [12] $\mathrm{z}_{f,s+1} = (\Gamma_i x_{i+j+1} + \mathrm{n}_{f,s+1})\, T$, where T is a square non-singular matrix.
Once the vector $\mathrm{z}_{f,s+1}$ is estimated, under the assumption that the system is observable, the estimation of the extended observability matrix can be realized, as in subsection 4.1, by estimating the propagator. Indeed, after an initial reorganization such that the first n rows of Γ_i are linearly independent, the following partition of the observation vector $\mathrm{z}_{f,s+1}$ can be introduced

$$\mathrm{z}_{f,s+1} = \begin{pmatrix} I_n \\ P^T \end{pmatrix} \Gamma_{i_1} x_{i+j+1} + \mathrm{n}_{f,s+1} = \begin{pmatrix} \mathrm{z}_{f_1,s+1} \\ \mathrm{z}_{f_2,s+1} \end{pmatrix} \begin{matrix} \} \in \mathbb{R}^{n\times 1} \\ \} \in \mathbb{R}^{(li-n)\times 1} \end{matrix}$$

where $\mathrm{z}_{f_1,s+1}$ and $\mathrm{z}_{f_2,s+1}$ are the components of $\mathrm{z}_{f,s+1}$ corresponding respectively to the n rows of Γ_{i_1} and $li - n$ rows of $\Gamma_{i_2} = P^T \Gamma_{i_1}$ (the same symbols are used before and after the reorganization, for the sake of simplicity). In the ideal noise-free case, it is easy to show that $\mathrm{z}_{f_2} = P^T \mathrm{z}_{f_1}$. In the presence of noise, this relation holds no longer. An estimate of P can however be obtained by minimizing the following cost function

$$V(P) = \mathbf{E}\|\mathrm{z}_{f_2} - P^T \mathrm{z}_{f_1}\|^2, \tag{3}$$

the uniqueness of $\hat{P}$ being ensured by the convexity of this criterion, which, in turn, can be guaranteed by suitable persistency of excitation assumptions [14]. Unfortunately, the LS solution of the optimization problem defined by (3) leads to a biased estimate, even when the residual vector is spatially and temporally white [12]. This difficulty can be circumvented by introducing an instrumental variable $\xi \in \mathbb{R}^{\gamma\times 1}$ ($\gamma \geq n$) in (3), assumed to be uncorrelated with the noise but sufficiently correlated with the state vector x, and by defining the new cost function

$$V_{IV}(P) = \mathbf{E}\|\mathrm{z}_{f_2}\xi^T - P^T \mathrm{z}_{f_1}\xi^T\|_F^2 \ .$$

Several algorithms have been developed to minimize this criterion depending on the number of instruments. In this paper, the EIVPM algorithm is considered due to its implementation straightforwardness and its low computational cost. This technique requires to construct an instrumental variable such that $\gamma > n$. By assuming that the input is sufficiently "rich" [14] so that $R_{\mathrm{z}_{f_1}\xi}$ is full rank, the asymptotic least squares estimate of the propagator is given by

$$\hat{P}^T = R_{\mathrm{z}_{f_2}\xi} R^{\dagger}_{\mathrm{z}_{f_1}\xi} \,. \tag{4}$$

Then, a recursive version of (4) can be obtained by adapting the overdetermined instrumental variable technique first proposed in [4]. The resulting algorithm is given by

$$\begin{aligned}
g_{s+1} &= \begin{pmatrix} R_{\mathrm{z}_{f_2,s}\xi_s}\xi_{s+1} & \mathrm{z}_{f_2,s+1} \end{pmatrix} \\
\Lambda_{s+1} &= \begin{pmatrix} -\xi_{s+1}^T\xi_{s+1} & \lambda \\ \lambda & 0 \end{pmatrix} \\
q_{s+1} &= R_{\mathrm{z}_{f_1,s}\xi_s}\xi_{s+1} \\
\Psi_{s+1} &= \begin{pmatrix} q_{s+1} & \mathrm{z}_{f_1,s+1} \end{pmatrix} \\
K_{s+1} &= \left(\Lambda_{s+1} + \Psi_{s+1}^T M_s \Psi_{s+1}\right)^{-1} \Psi_{s+1}^T M_s \\
P_{s+1}^T &= P_s^T + (g_{s+1} - P_s^T\Psi_{s+1})K_{s+1} \\
R_{\mathrm{z}_{f_1,s+1}\xi_{s+1}} &= \lambda R_{\mathrm{z}_{f_1,s}\xi_s} + \mathrm{z}_{f_1,s+1}\xi_{s+1}^T \\
R_{\mathrm{z}_{f_2,s+1}\xi_{s+1}} &= \lambda R_{\mathrm{z}_{f_2,s}\xi_s} + \mathrm{z}_{f_2,s+1}\xi_{s+1}^T \\
M_{s+1} &= \frac{1}{\lambda^2}(M_s - M_s\Psi_{s+1}K_{s+1}) \,,
\end{aligned}$$

where $0 < \lambda \leq 1$ is a forgetting factor and $M_{s+1} = \left(R_{\mathrm{z}_{f_1,s+1}\xi_{s+1}} R^T_{\mathrm{z}_{f_1,s+1}\xi_{s+1}}\right)^{-1}$.

5 Simulation examples

In this section, some properties of the recursive algorithms are studied by use of simulations. We start from a fourth order model with one input and one output. Its system matrices are equal to

$$\begin{aligned}
A &= \begin{pmatrix} 0.67 & 0.67 & 0 & 0 \\ -0.67 & 0.67 & 0 & 0 \\ 0 & 0 & -0.67 & -0.67 \\ 0 & 0 & 0.67 & -0.67 \end{pmatrix}, \qquad B = \begin{pmatrix} 0.6598 \\ 1.9698 \\ 4.3171 \\ -2.6436 \end{pmatrix}, \\
C &= \begin{pmatrix} -0.5749 & 1.0751 & -0.5225 & 0.1830 \end{pmatrix}, \quad D = -0.7139 \,.
\end{aligned} \tag{5}$$

The measurement and process noise are respectively equal to $w_k = Ke_k$ and $v_k = Ge_k$, where

$$K = \begin{pmatrix} -0.1027 \\ 0.5501 \\ 0.3545 \\ -0.5133 \end{pmatrix}, \; G = 0.9706 \text{ and } e_k \text{ is white Gaussian noise with variance } \sigma_e^2. \tag{6}$$

There are two vibration modes. The first mode has eigenfrequency equal to $f_1 = 4.0094$Hz and damping ratio $\zeta_1 = 6.8472\%$, while the second mode has eigenfrequency $f_2 = 12.0031$Hz and damping ratio $\zeta_2 = 2.2872\%$. The sampling frequency is equal to $f_s = 32$ Hz and we simulate three minutes.
In Section 5.1 we simulate time-varying damping ratios and examine the tracking capabilities of the recursive subspace algorithms. In Section 5.2 we look at the effects of an overestimation of the model order.

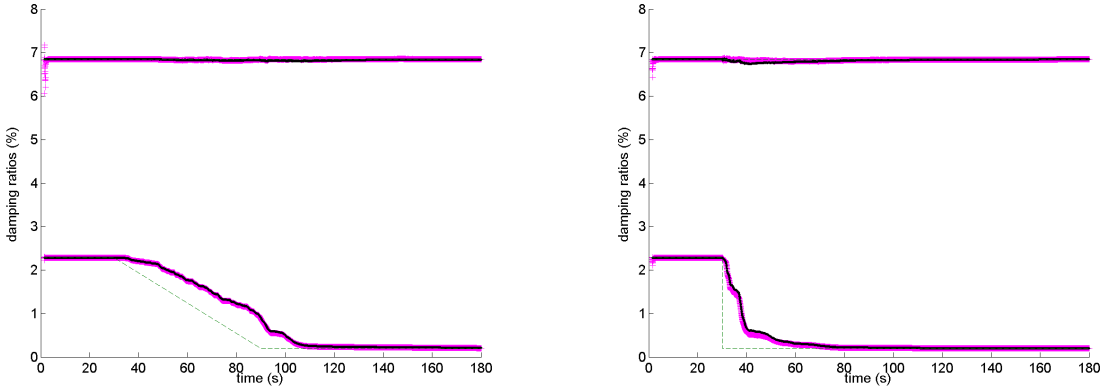

(a) Estimating a linearly varying damping ζ_2. (b) Estimating an abruptly varying damping ζ_2.

Figure 1: The estimated dampings for Case 1: noiseless simulation ($\sigma_e = 0$) and estimation with forgetting factor $\lambda = 0.999$. The green dashed lines represent the correct values, the black dots the results obtained with RPM2, the magenta plus signs show the results of EIVPM.

5.1 Tracking a time-varying damping ratio

In this section the tracking capabilities of the recursive algorithms that were discussed in Section 4.1 and Section 4.2, are evaluated. The parameters used in the estimation are the following: the model order is $n = 4$ and $i = 8$. The PO MOESP scheme is used in the RPM2 algorithm and the instrumental variable in EIVPM is chosen as $\xi_s = \begin{pmatrix} \mathrm{u}_{p,s}^T & \mathrm{y}_{p,s}^T \end{pmatrix}^T$. To initialize the recursive algorithms, the first 47 simulated data points (less than two seconds) are used to identify a model with the non-recursive subspace algorithm com_stat [18].
Two types of time-varying dampings are considered: first, a linearly varying damping (ζ_2 goes from 2.2872% to 0.2% between 30s and 90s) and second, an abrupt drop of the damping ratio (ζ_2 drops from 2.2872% to 0.2% at 30s). A decreasing damping is a not uncommon phenomenon during in-flight tests and usually a reason for concern.
Four scenarios are simulated, in which the noise variance σ_e^2 and the forgetting factor λ are varied.

Case 1: $\sigma_e^2 = 0$ and $\lambda = 0.999$
This is the noiseless, purely deterministic case, with a forgetting factor λ close to one. The frequencies are estimated perfectly and the estimated dampings are shown in Figure 1. There is a delay in tracking the varying damping ratios, which is due to the large forgetting factor. Indeed, the larger λ, the slower the algorithms forget past data.

Case 2: $\sigma_e^2 = 0$ and $\lambda = 0.9$
The forgetting factor in the identification algorithms is decreased to 0.9. This means that the past data become less important compared to Case 1. Consequently, the algorithms are much more able to track the changes. This can be seen in Figure 2.

Case 3: $\sigma_e^2 = 10$ and $\lambda = 0.9$
The process and measurement noise sources $w_k = Ke_k$ and $v_k = Ge_k$ are introduced, where e_k has variance $\sigma_e^2 = 10$. Using the 'small' forgetting factor $\lambda = 0.9$, leads to very bad estimates for the damping ratios, as is shown in Figure 3.

Case 4: $\sigma_e^2 = 10$ and $\lambda = 0.999$
Increasing the forgetting factor to $\lambda = 0.999$, gives much better damping estimates when $\sigma_e^2 = 10$, which can be seen Figure 4. Note that estimating the constant damping ratio ζ_1 has become more difficult than in the noiseless case. The frequencies, on the other hand, are estimated very well.

It is clear from this example that there is a trade-off in the choice of the estimation parameters. Decreasing the forgetting factor makes the recursive algorithms react faster, but also makes them more sensitive to noise, which influences the damping ratio estimates very much.

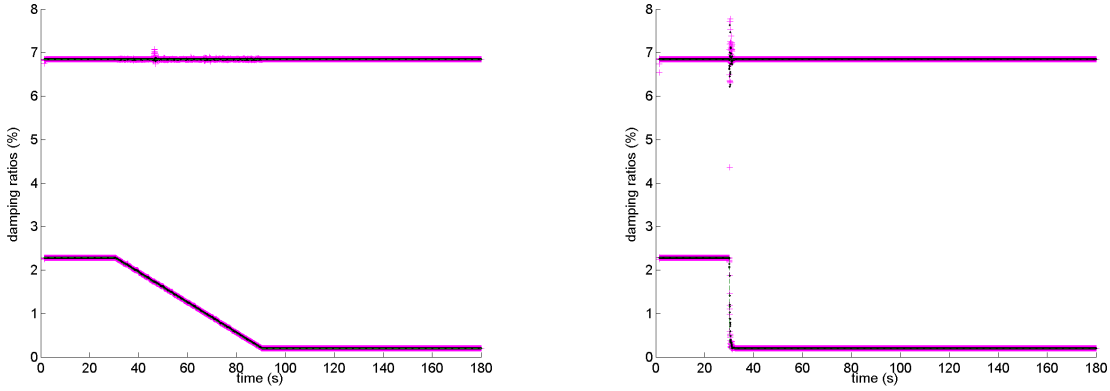

(a) Estimating a linearly varying damping ζ_2. (b) Estimating an abruptly varying damping ζ_2.

Figure 2: The estimated dampings for Case 2: noiseless simulation ($\sigma_e = 0$) and estimation with forgetting factor $\lambda = 0.9$. The green dashed lines represent the correct values, the black dots the results obtained with RPM2, the magenta plus signs show the results of EIVPM.

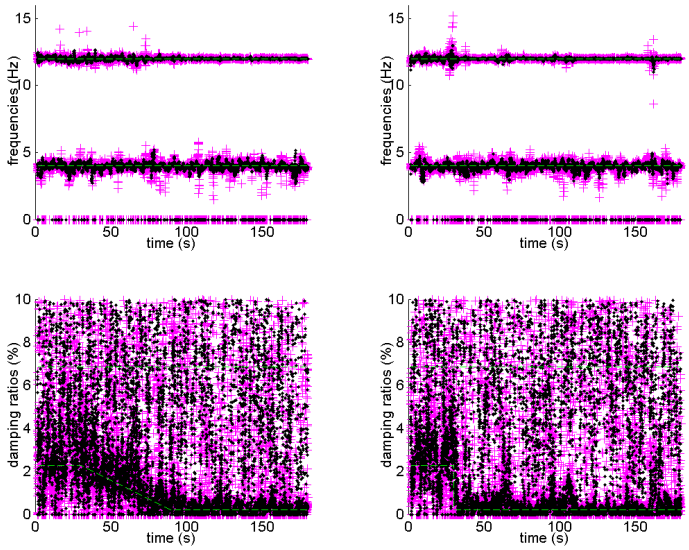

Figure 3: The estimated frequencies and dampings for Case 3: noisy simulation ($\sigma_e = 10$) and estimation with forgetting factor $\lambda = 0.9$. The left column shows the results for a linearly varying damping ζ_2, the right column for an abrupt change of ζ_2. On top, the frequencies are given, the bottom figures show the damping ratios. The green dashed lines represent the correct values, the black dots the results obtained with RPM2, the magenta plus signs show the results of EIVPM.

5.2 Overestimation of the model order

In the previous section, we assumed that the order of the system was known. In practice, however, this is often not the case. For the in-flight data, we have to choose an order which is large enough to incorporate all important vibration modes. Therefore, the influence of overestimating the model order is studied.

The same fourth order system as in Section 5.1 is simulated, but without time-varying damping. The system matrices are given in (5) and (6) and we simulate with $\sigma_e^2 = 10$. The estimation parameters are chosen as follows: $n = 6$, $i = 12$ and the first 71 data points are used for the initialization. Since there is no time-variance in the simulated system, we take the forgetting factor $\lambda = 1$. The estimated frequencies and damping ratios are shown in Figure 5. By choosing $n = 6$, we are able to identify three modes. However, only frequencies and dampings are computed from poles of the identified discrete-time system that appear

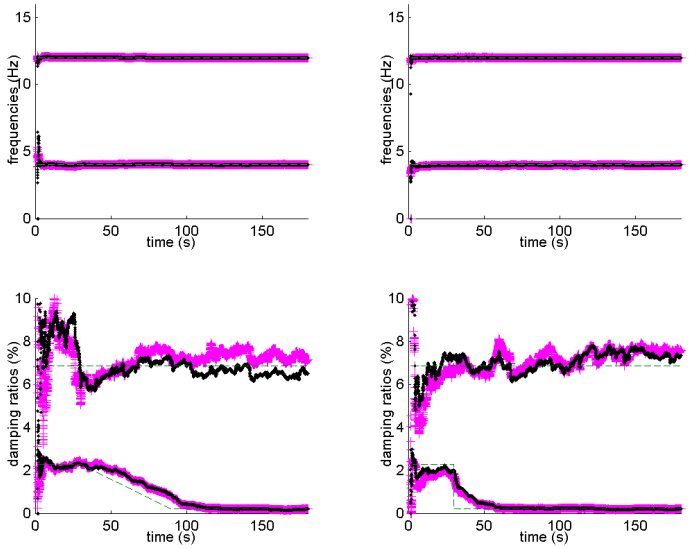

Figure 4: The estimated frequencies and dampings for Case 4: noisy simulation ($\sigma_e = 10$) and estimation with forgetting factor $\lambda = 0.999$. The left column shows the results for a linearly varying damping ζ_2, the right column for an abrupt change of ζ_2. On top, the frequencies are given, the bottom figures show the damping ratios. The green dashed lines represent the correct values, the black dots the results obtained with `RPM2`, the magenta plus signs show the results of `EIVPM`.

as complex conjugate pairs within the unit circle. That explains why at many time points, less than three frequencies and dampings per identification method can be seen.
The true 'physical' frequencies and damping ratios are estimated very well by both methods. As observed in [11], the variance of the 'non-physical' estimated poles is larger than that of the 'physical' poles. This will be used to introduce a new kind of stabilization diagram in Section 6.

6 Applying recursive algorithms to in-flight data

In this section, the recursive algorithms of Section 4 are applied to measurements on airplanes during flight tests. In Section 6.1 the data are described, in Section 6.2 the identification results are given and in Section 6.3 we discuss the computational speed of the applied identification algorithms.

6.1 Description of the data

The FliTE consortium (see Acknowledgments) provided a dataset of in-flight tests executed an a real aircraft. Data were acquired at five different flight conditions (#1, #2, #3, #4, #5). The excitation signal, applied by the pilot, was a narrow band 0–60Hz white noise. Responses were acquired through twelve accelerometers at a 256Hz sampling frequency. For more information on the data, we refer to [19, 20], where other (non-recursive) identification methods were applied to the same dataset.
The data are preprocessed in the following way. The data are lowpass filtered and downsampled with a factor 8 because all relevant information is available below 16Hz. In that way, the sampling frequency becomes 32Hz. We discard noisy output signals, whose coherence with the input is too small. For flight points #1, #2 and #4, the fifth and seventh output are not taken into account, while for flight points #3 and #5, outputs one, three, five and seven are discarded.
The parameters in the identification methods are chosen as follows: $n = 16$ and $i = 4$. Because the flight points represent time-invariant conditions, the forgetting factor was taken equal to $\lambda = 1$ (no forgetting).

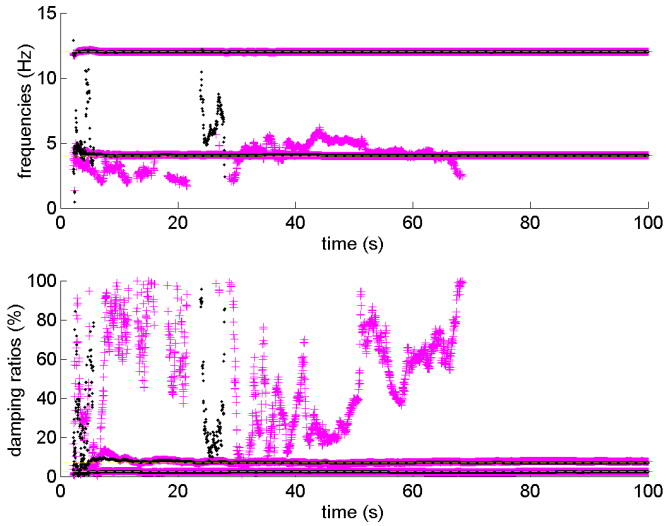

Figure 5: The estimated frequencies (top) and damping ratios (bottom) when the order of the model ($n = 6$) is larger than the true system order ($n = 4$). The yellow dashed lines represent the correct values, the black dots the results obtained with RPM2, the magenta plus signs show the results of EIVPM.

The PO MOESP scheme is used in the RPM2 algorithm and the instrumental variable in EIVPM is chosen as $\xi_s = \begin{pmatrix} u_{p,s}^T & y_{p,s}^T \end{pmatrix}^T$. For flight points #1, #2 and #4, where 10 outputs are available, 95 data points are used to initialize the model with the non-recursive algorithm com_stat, while for flight points #3 and #5, with 8 outputs, 79 data points are used for the initialization. At every time step the models obtained with the two recursive methods RPM2 and EIVPM are updated. Their results are compared to the results obtained with the non-recursive algorithm com_stat, which estimates a new model every 32 data points, i.e. once every second. It uses all available measurements up to that point to estimate a new model.

6.2 Identification results

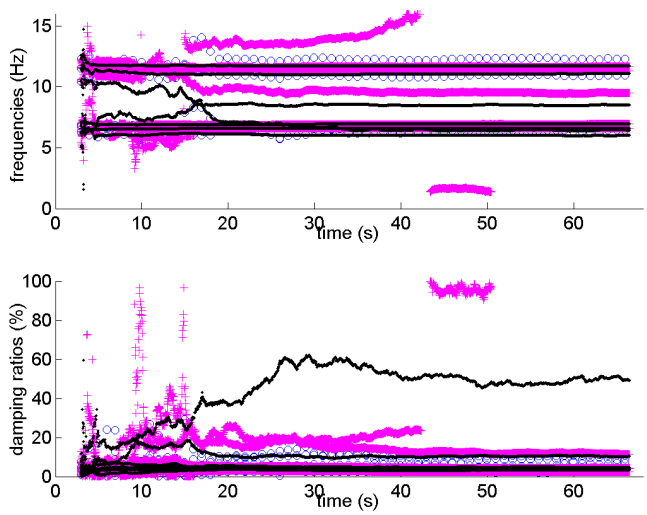

Figure 6: The estimated frequencies (top) and dampings (bottom) for flight point #1. The black dots represent the results obtained with RPM2, the magenta plus signs show the results of EIVPM and the blue circles those of the non-recursive com_stat.

For all five flight points models were identified recursively. The modal frequencies and damping ratios

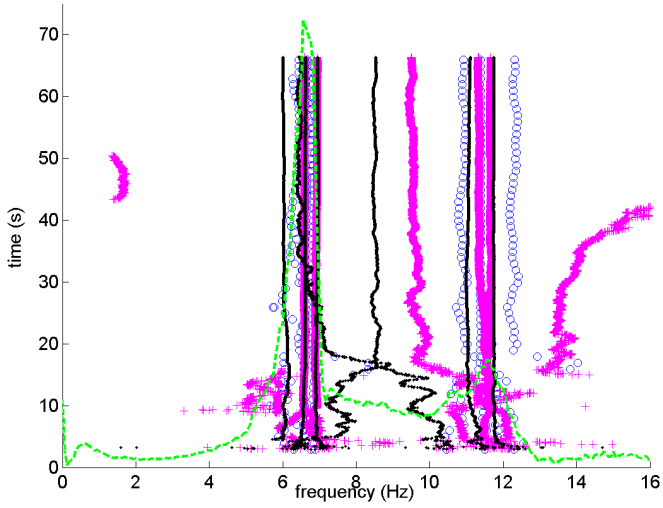

Figure 7: The stabilization diagram for flight point #1. The black dots represent the results obtained with RPM2, the magenta plus signs show the results of EIVPM and the blue circles those of the non-recursive com_stat. The green dashed line represents the FRF of the input and fourth output.

obtained from the data in flight point #1 are shown in Figure 6 as a function of time. Many frequency and damping estimates converge in time. Some estimates disappear after some time, while others show a higher variance than the converging estimates over time. Both effects are due to the overestimation of the model order, as explained in Section 5.2. Following the terminology often used in vibration mode analysis, the converging modes can be called 'physical modes', while the others are 'mathematical modes'. Furthermore, we introduce here a new type of stabilization diagram, where the x-axis is frequency and the y-axis is *not* the model order, as in common stabilization diagrams (see e.g. [19, 20]), but time. In Figure 7 the stabilization diagram for the first flight point is shown. The green dashed line represents a non-parametric estimate of the transfer function (FRF) from the input to the fourth output.

The final values of the stabilized, 'physical' frequencies and damping ratios for the five flight points are given in Table 1. Note that the damping ratios corresponding to some stabilized frequencies did not stabilize. The results for these modes were not included in Table 1. The frequencies and damping ratios obtained are similar to those reported in [19, 20].

Several observations can be made:

- The stabilization diagrams of the non-recursive algorithm com_stat are more difficult to interpret than those of the recursive algorithms.

	flight point #1		flight point #2		flight point #3		flight point #4		flight point #5	
	f (Hz)	ζ (%)	f (Hz)	ζ (%)	f (Hz)	ζ (%)	f (Hz)	ζ (%)	f (Hz)	ζ (%)
RPM2	6.0116	3.5815	5.9581	4.5295	6.6710	1.8541	6.1739	14.3069	6.6265	2.6188
	6.6235	3.7528	6.7232	2.9545	6.7756	7.3267	6.6669	5.8640	6.7398	5.7286
	6.9564	3.6494	6.8227	5.0781	7.4701	12.7308	6.7506	1.2581	7.0437	21.0211
	8.5265	10.4214	7.4480	22.5484	11.4220	3.6722	9.1797	12.8608	11.0306	4.1329
	11.1040	4.7235	11.1762	7.5918	12.3259	3.1036	10.8343	8.6058	11.5147	1.8748
	11.7505	3.4432	11.6339	4.7289			11.5777	3.9094	12.5687	3.3231
EIVPM	6.5891	4.0818	6.8084	2.8753	6.6045	5.1471	6.5380	4.9126	6.5654	6.3881
	6.9411	2.3670	11.3809	3.5252	6.7449	1.6147	6.7656	1.2370	6.6689	2.0430
	9.4888	11.3808	11.5954	5.4129	10.9731	5.7992	10.9263	5.7984	11.4863	5.1401
	11.3188	4.1065			11.5553	3.0436	11.6006	3.9410	12.5857	2.9964
	11.6613	4.4686			12.7096	3.0437				

Table 1: The estimated frequencies (f) and damping ratios (ζ) for all flight points using two recursive subspace identification methods RPM2 and EIVPM.

- Algorithm RPM2 tends to give more stabilized modes than EIVPM. In flight point #2, e.g., EIVPM only finds three stabilized modes, while RPM2 finds six.
- Not every mode is detected in each flight point. For example, algorithm RPM2 finds a mode around 6Hz in flight points #1, #2 and #4, but not in flight points #3 and #5.
- Damping ratio estimates corresponding to the same frequency sometimes differ much from flight point to flight point. For example, in flight point #3 the mode with frequency around 6.7Hz, identified by RPM2, has damping ratio 7.33%, while in flight point #4 it is only 1.26%.
- It is not always easy to decide which mode in one flight point corresponds to which in another flight point. It would be advantageous to track the frequencies and dampings in between the different flight points. This is exactly the aim of future in-flight tests, when also data will be measured during the transition from one flight point to the following.

6.3 Computational speed

In Figure 8 we show the time needed to process 96 new data points as a function of time. Note that com_stat only updates the model every 32 points, while EIVPM and RPM2 do this every time a new data point is available. Therefore, the blue circles in Figure 8 represent the computation cost for 3 updates of the com_stat model and for 96 updates of the other two models. The computation time for com_stat increases linearly with time (i.e. with the number of data points used for the identification). On the other hand, the time needed to update the models by means of the recursive methods, remains constant.
It is clear from Figure 8 that the data can be processed in real-time. For com_stat it might become more difficult when longer data sequences are given. In this case, memory problems could arise too. A solution for these problems could be to use a sliding window that discards the data points that lie furthest in the past. The recursive algorithms EIVPM and RPM2 do not have these problems.

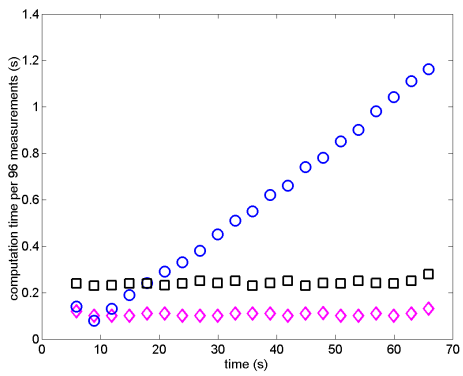

Figure 8: The time needed to process 96 new data points as a function of time. The black squares represent the time needed by RPM2 for 96 model updates, the magenta diamonds the computation time for 96 updates by EIVPM and the blue circles the time needed for 3 identifications by the non-recursive com_stat.

7 Conclusions and future work

In this paper two recent recursive subspace identification algorithms are studied. Simulation examples show that the algorithms are able to track changing damping ratios, provided that for noisy measurements the forgetting factor is chosen large enough (not much forgetting). The algorithms are also applied to in-flight measurements on an airplane. Using measurements from five flight points, several modes (eigenfrequencies and damping ratios) of the airplane are identified. The computation time is short enough to apply the methods

on-line.
However, several issues need to be looked at in the future. The entire dataset was used to decide which outputs could be discarded. This is not possible when working on-line. It will be investigated if keeping the data from the noisy outputs deteriorates the identification results much. We also used the whole dataset to decimate the data (lowpass filtering followed by downsampling). This must be done on-line too.
In the near future measurements from the transition in between flight points will become available. The methods described in this paper, will be applied to these data. By tracking the modal parameters, it should be much easier to decide which frequencies and dampings correspond to the same modes in the different flight points.
It would be interesting to have a recursive subspace identification algorithm based on the propagator concept, for the purely stochastic identification problem, i.e. one without measured input. When the input applied by the pilot falls away, one should be able to switch to the stochastic method and keep tracking the modal parameters.
It would also be very useful to have confidence bounds on the identified modal frequencies and damping ratios. To the best of our knowledge they do not even exist for non-recursive subspace algorithms.

Acknowledgments

Research supported by Research Council K.U.Leuven: GOA AMBioRICS, CoE EF/05/006 Optimization in Engineering, several PhD/postdoc & fellow grants; Flemish Government: FWO: PhD/postdoc grants, projects, G.0407.02 (support vector machines), G.0197.02 (power islands), G.0141.03 (Identification and cryptography), G.0491.03 (control for intensive care glycemia), G.0120.03 (QIT), G.0452.04 (new quantum algorithms), G.0499.04 (Statistics), G.0211.05 (Nonlinear), G.0226.06 (cooperative systems and optimization), G.0321.06 (Tensors), G.0553.06 (VitamineD), research communities (ICCoS, ANMMM, MLDM); IWT: PhD Grants,GBOU (McKnow), Eureka-FliTE2; Belgian Federal Science Policy Office: IUAP P5/22 ('Dynamical Systems and Control: Computation, Identification and Modelling', 2002-2006) ; PODO-II (CP/40: TMS and Sustainability); EU: FP5-Quprodis; ERNSI; Contract Research/agreements: ISMC/IPCOS, Data4s, TML, Elia, LMS, Mastercard

References

[1] M. Basseville, A. Benveniste, M. Goursat, L. Hermans, L. Mevel, and H. Van der Auweraer, *Output-only subspace-based structural identification: from theory to industrial testing practice*, Journal of Dynamic Systems, Measurement, and Control, Vol. 123, No. 4 (2001), pp. 668–676.

[2] Y. M. Cho, G. Xu, and T. Kailath, *Fast recursive identification of state space models via exploitation displacement structure*, Automatica, Vol. 30, No. 1 (1994), pp. 45–60.

[3] K. De Cock, B. Peeters, A. Vecchio, H. Van der Auweraer, and B. De Moor, *Subspace system identification for mechanical engineering*, in *Proceedings of the International Conference on Noise and Vibration Engineering (ISMA 2002)*, Leuven, Belgium (2002).

[4] B. Friedlander, *The overdetermined recursive instrumental variable method*, IEEE Transactions on Automatic Control, Vol. 4 (1984), pp. 353–356.

[5] I. Goethals, L. Mevel, A. Benveniste, and B. De Moor, *Recursive output only subspace identification for in-flight flutter monitoring*, in *Proceedings of the 22nd International Modal Analysis Conference (IMAC-XXII)*, Dearborn, Michigan (2004).

[6] G. H. Golub and C. F. Van Loan, *Matrix computations*, John Hopkins University Press, Baltimore MD, 3rd edition (1996).

[7] T. Gustafsson, *Recursive system identification using instrumental variable subspace tracking*, in *Proceedings of the 11th IFAC Symposium on System Identification (SYSID 1997)*, Fukuoka, Japan (1997).

[8] L. Hermans and H. Van der Auweraer, *Modal testing and analysis of structures under operational conditions: industrial applications*, Mechanical Systems and Signal Processing, Vol. 13, No. 2 (1999), pp. 193–216.

[9] H. Krim and M. Viberg, *Two decades of array signal processing research: the parametric approach*, IEEE Signal Processing Magazine, Vol. 13 (1996), pp. 67–94.

[10] M. Lovera, T. Gustafsson, and M. Verhaegen, *Recursive subspace identification of linear and non-linear Wiener state-space models*, Automatica, Vol. 36 (2000), pp. 1639–1650.

[11] G. Mercère, *Contribution à l'identification récursive des systèmes par l'approche des sous-espaces*, PhD thesis, Université des Sciences et Technologies de Lille, Villeneuve d'Ascq, France (2004).

[12] G. Mercère, S. Lecœuche, and M. Lovera, *Recursive subspace identification based on instrumental variable unconstrained quadratic optimization*, International Journal of Adaptive Control and Signal Processing, Vol. 18 (2004), pp. 771–797.

[13] G. Mercère, S. Lecœuche, and C. Vasseur, *A new recursive method for subspace identification of noisy systems: EIVPM*, in *Proceedings of the 13th IFAC Symposium on System Identification*, Rotterdam, The Netherlands (2003).

[14] G. Mercère and M. Lovera, *Convergence analysis of instrumental variable recursive subspace identification algorithms*, in *Proceedings of the 14th IFAC Symposium on System Identification*, Newcastle, Australia (2006).

[15] J. Munier and G. Y. Delisle, *Spatial analysis using new properties of the cross spectral matrix*, IEEE Transactions on Signal Processing, Vol. 39 (1991), pp. 746–749.

[16] H. Oku and H. Kimura, *Recursive 4SID algorithms using gradient type subspace tracking*, Automatica, Vol. 38 (2002), pp. 1035–1043.

[17] B. Peeters and G. De Roeck, *Reference-based stochastic subspace identification for output-only modal analysis*, Mechanical Systems and Signal Processing, Vol. 13, No. 6 (1999), pp. 855–878.

[18] P. Van Overschee and B. De Moor, *Subspace Identification for linear systems: Theory – Implementation – Applications*, Kluwer Academic Publishers, Dordrecht, The Netherlands (1996).

[19] A. Vecchio, B. Peeters, and H. Van der Auweraer, *Application of advanced parameter estimators to the analysis of in-flight measured data*, in *Proceedings of the 20th International Modal Analysis Conference (IMAC XX)*, Los Angeles, CA (2002).

[20] A. Vecchio, M. Scionti, B. Peeters, and H. Van der Auweraer, *Modal parameters extraction from in-flight measured data for critical flutter airspeed identification*, in *Proceedings of the International Conference on Noise and Vibration Engineering (ISMA2002)*, Leuven, Belgium (2002).

[21] M. Verhaegen, *Identification of the deterministic part of MIMO state space models given in innovations form from input-output data*, Automatica, Vol. 30, No. 1 (1994), pp. 61–74.

[22] M. Verhaegen and E. Deprettere, *A fast, recursive MIMO state space model identification algorithm*, in *Proceedings of the 30th IEEE Conference on Decision and Control* (1991), pp. 1349–1354.

[23] M. Verhaegen and P. Dewilde, *Subspace model identification part 1. The output-error state-space model identification class of algorithms*, International Journal of Control, Vol. 56, No. 5 (1992), pp. 1187–1210.

[24] M. Verhaegen and P. Dewilde, *Subspace model identification part 2. Analysis of the elementary output-error state-space model identification algorithm*, International Journal of Control, Vol. 56, No. 5 (1992), pp. 1211–1241.

[25] M. Verhaegen, *Subspace model identification part 3. Analysis of the ordinary output-error state-space model identification algorithm*, International Journal of Control, Vol. 56, No. 3 (1993), pp. 555–586.

[26] M. Viberg, *Subspace based methods for the identification of linear time invariant systems*, Automatica, Vol. 31 (1995), pp. 1835–1851.

[27] B. Yang, *Projection approximation subspace tracking*, IEEE Transactions on Signal Processing, Vol. 43, No. 1 (1995), pp. 95–107.